

Title: MRAnnotator: A Multi-Anatomy Deep Learning Model for MRI Segmentation

^{1,†}Alexander Zhou, ^{1,†}Zelong Liu, ¹Andrew Tieu, ¹Nikhil Patel, ²Sean Sun, ²Anthony Yang, ²Peter Choi, ¹Valentin Fauveau, ¹George Soultanidis, ²Mingqian Huang, ²Amish Doshi, ^{1,2}Zahi A. Fayad, ^{3,4}Timothy Deyer, ¹Xueyan Mei

¹BioMedical Engineering and Imaging Institute, Icahn School of Medicine at Mount Sinai, New York, NY

²Department of Diagnostic, Molecular, and Interventional Radiology, Icahn School of Medicine at Mount Sinai, New York, NY

³East River Medical Imaging, New York, NY

⁴Department of Radiology, Cornell Medicine, New York, NY

[†]These authors contributed equally to this work.

Corresponding author: Xueyan Mei, email: xueyan.mei@icahn.mssm.edu.

ABSTRACT

Purpose

To develop a deep learning model for multi-anatomy and many-class segmentation of diverse anatomic structures on MRI imaging.

Materials and Methods

In this retrospective study, two datasets were curated and annotated for model development and evaluation. An internal dataset of 1022 MRI sequences from various clinical sites within a health system and an external dataset of 264 MRI sequences from an independent imaging center were collected. In both datasets, 49 anatomic structures were annotated as the ground truth. The internal dataset was divided into training, validation, and test sets and used to train and evaluate an nnU-Net model. The external dataset was used to evaluate nnU-Net model generalizability and performance in all classes on independent imaging data. Dice scores were calculated to evaluate model segmentation performance.

Results

The model achieved an average Dice score of 0.801 on the internal test set, and an average score of 0.814 on the complete external dataset across 49 classes.

Conclusion

The developed model achieves robust and generalizable segmentation of 49 anatomic structures on MRI imaging. A future direction is focused on the incorporation of additional anatomic regions and structures into the datasets and model.

Introduction

MRI has become an essential diagnostic tool due to its ability to provide high-resolution 3D medical imaging, with vast amounts of imaging data and associated medical data generated annually. With recent advances in machine learning and computational power over the last decade, there has been significant research interest in applying deep learning techniques to MRI and other modalities to enhance radiological workflows (1,2). Of these workflows, medical image segmentation is particularly crucial for both clinical and research applications, such as disease quantification, abnormality detection, therapy planning, dataset curation, and artificial intelligence model development (3,4). The creation of automated segmentation models thus has the potential to reduce radiological workloads, improve diagnostic accuracy, enhance radiologist capabilities, and accelerate machine learning research applied to radiology (5).

A key bottleneck in the development of these models is the limited availability of annotated medical imaging data for model training. This arises due to the need for annotations by trained medical experts, privacy regulations, relative scarcity of particular pathologies, and resource intensity (6,7). An emerging paradigm that can alleviate this bottleneck is the development of foundation models, which are artificial intelligence models trained on massive, diversified datasets that can be adapted to new downstream tasks with limited or no additional data. However, this paradigm is still limited in medical imaging, due to domain complexities and limited availability of large-scale diversified medical datasets, with most current medical imaging models developed with a task-specific paradigm that only enables the execution of narrowly defined tasks (8).

Recently, Zhang and Metaxas proposed the concept of a “spectrum of foundation models” that spans the range of general vision, medical, modality-specific, and organ/task-specific foundation models. This would enable the selection and adaptation of the most appropriate foundation model for a downstream task with minimal training samples and compute power. Furthermore, the development of diverse foundational models would enable the eventual merging of complementary datasets to build larger and more unified datasets and foundation models (9).

Towards addressing this need, we aimed to develop a modality-specific model that is able to accomplish many-class 3D anatomic segmentation on MRI imaging data with robust performance in various anatomic regions (MRAnnotator). Following the approach established by Wasserthal et al in developing TotalSegmentator for CT (10), we trained MRAnnotator on a large, diversified internal MRI dataset, and we demonstrated generalizability of our model on a parallel external dataset from a separate medical center. Furthermore, we demonstrate the utility of our MRI model by using our model’s pretrained weights and benchmarking on several well-known public datasets.

Materials and Methods

This retrospective study was performed in accordance with relevant local and national regulations and approved by STUDY-22-00465 at Mount Sinai. The requirement to obtain individual informed consent was waived.

Dataset Curation

Two datasets were curated and annotated for this study. The first dataset consisted of studies from the Mount Sinai Health System (MSHS) for the training, validation, and testing of MRAnnotator (“internal dataset”). The second dataset consisted of studies from East River Medical Imaging (ERMI) for the testing of model generalizability (“external dataset”).

Internal dataset. To produce a robust and diversified site dataset for model development, 849 patients with 1022 MRI sequences were randomly sampled between 2010 and 2023 from the MSHS PACS across six clinical sites across New York, NY. The final dataset of 1022 MRI sequences was divided into training, validation, and test sets by patient. The holdout test set consisted of 240 MRI patients (30 patients and all associated sequences for each of the 8 anatomic regions annotated). The remaining 782 sequences were randomly split with a 4:1 training:validation ratio, for a training set of 625 sequences and a validation set of 157 sequences (**Fig 1A**).

External dataset. 248 patients were randomly sampled from 2006-2022 from the ERMI PACS. ERMI was selected as a completely independent clinical center for external testing. The same process of sequence selection was conducted on these patients, for a total of 264 MRI studies. The same post-processing was conducted to produce the final dataset of 264 MRI studies. This entire dataset was designated as a holdout test set for external validation (**Fig 1A**).

Dataset Annotation

49 anatomic structures in 8 anatomic regions were segmented in both datasets (**Table 1**). Segmentation was conducted by medical students (annotators), with supervision from senior radiologists, both of whom approved and corrected all annotations as needed. The Discovery Viewer platform was used for manual segmentation, as well as the generation and manual correction of intermediate annotation model segmentations (11).

To speed up the annotation process, we adopted an iterative model-assisted workflow similar to that of Wasserthal et al for all non-vertebral anatomic structures (10). 10 initial sequences were manually segmented by annotators and used to train a preliminary nnU-Net model (3). This was used to generate intermediate segmentations on 10 more sequences, with manual correction and refinement by annotators as needed. The intermediate annotation model was then retrained on all 20 sequences. This correction and retraining process was repeated with 40 and 60 total sequences, then used to generate intermediate segmentations for all 578 non-vertebral sequences. For vertebral anatomic structures (C3-C7, T1-T12, L1-L5), annotators used MedSAM (12) to generate intermediate segmentations from bounding boxes for all 444 vertebral sequences. MedSAM was used for this task due to its ability to segment the relatively well-defined and higher-contrast vertebral bodies. All 1022 sequences were ultimately manually reviewed and corrected by annotators, with final review and correction by supervisors. These finalized annotations served as the ground truth for model training and internal/external evaluation.

Model Training

The final MRAnnotator model uses a 3D nnU-Net architecture, which self-configures parameters based on dataset properties and hardware conditions (3) and has achieved robust performance in diverse medical

imaging applications (10,13,14). This model was trained on the finalized internal dataset independently of the intermediate annotation models. For the configuration of training strategy, we manually disabled mirroring for data augmentation to help the model learn laterality of 3D volumes (e.g., differentiating right vs. left structures). The model was trained with 4000 epochs, and the model weights with the highest Dice score on the validation dataset were saved as the finalized model for evaluation.

Model Evaluation and Statistical Analysis

Internal and external dataset performance. The Dice similarity coefficient, which measures spatial overlap accuracy, was used to evaluate model-predicted segmentations compared to the corresponding human-finalized ground truth segmentations (15). The Dice coefficient symmetrically penalizes non-overlapping regions, with a coefficient of 0 indicating no overlap and 1 indicating perfect overlap.

Model performance was evaluated on the holdout test set from the internal dataset (240 patients, 30 patients per anatomic region), which is not seen by the model during training nor used for hyperparameter tuning. Model performance on all anatomic segmentation classes was also evaluated on the external dataset, which was annotated with the same anatomic classes. The entire external dataset was also used as a holdout test set, and not seen by the model during training.

We evaluated the distribution of Dice coefficients for each anatomic structure via the Shapiro-Wilk test. If the data was normally distributed, we calculated the 95% confidence interval (CI) for the Dice coefficient using the central limit theorem. If not, we used a bootstrapping method involving 1,000 resamples to calculate the 95% CI.

Results

Segmentation Evaluation

MRAnnotator achieved a total average Dice score of 0.801 on the internal dataset holdout test set, and 0.814 on the external dataset. Results for each anatomic structure class on the internal and external datasets are shown in **Table S1**. The performance across each anatomy is summarized in **Table 1**. Examples of model segmentation are shown in **Fig 2**. Given the characteristic differences between the internal and external datasets, this demonstrates robust generalizability of our model across all structures.

Table 1. Dice scores for each anatomical region within the internal and external datasets, and the overall average dice score of 49 labels on internal test dataset and 47 labels on external test dataset.

Anatomy	Average Internal Dice score	Average External Dice score
Abdomen	0.790	0.776*
Pelvis	0.932	0.860
Prostate	0.951	0.839
Shoulder	0.880	0.937
Knee	0.879	0.878

Cervical spine	0.855	0.835
Thoracic spine	0.728	0.742
Lumbar spine	0.641	0.809
Overall average	0.801	0.814

*Due to varying protocols, the ERMI data was not optimized for the stomach and esophagus, leading to the exclusion of these two labels from the annotation.

Discussion

In this study, we trained a robust model, MRAnnotator, on a diversified dataset of 1022 MRI sequences that is able to segment 49 anatomic structures across several distinct anatomic regions. Our model achieved high accuracy across all classes on both internal and external test data, demonstrating strong generalizability. Furthermore, we demonstrated the ability of our model to improve performance on several well-established datasets, highlighting the flexibility of MRAnnotator for diverse downstream tasks.

There has been limited research exploring the development of a model for many-structure MRI segmentation across multiple anatomic regions, despite the current availability of relatively large-scale MRI datasets for brain (16–18), abdomen (19,20), pelvis (21), and cardiac (22). Multi-class models trained on these datasets have achieved high performance but have been limited by the number of structures labeled and the anatomic region contained within an individual dataset. For example, Ding et al recently proposed and trained a novel state-of-the-art self-supervised few-shot segmentation architecture on the Combined Healthy Abdominal Organ Segmentation CT/MRI dataset (19), and their model was limited to only four structures (23). Similarly, Kondo and Kasai trained a residual U-Net with deep supervision for CT/MRI segmentation of abdominal organs on the AMOS dataset (20), which was limited to 15 abdominal structures (24).

Thus, there is a clear gap to demonstrate the feasibility of training more generalized MRI segmentation models that can serve as an out-of-the-box tool or starting point for more downstream tasks. Towards this goal, our annotated dataset serves as a standardized and diversified many-class many-anatomy dataset for the development of these models. Furthermore, the segmentation performance of MRAnnotator on its 49 anatomic structures demonstrates the viability of this approach and paves the way for the development of broader foundation models that can incorporate even more anatomies, modalities, and/or tasks.

We believe that MRAnnotator has many potential applications. As an out-of-the-box tool, our model can be used in a model-assisted annotation workflow for the curation of larger datasets from existing unlabeled images, as part of a broader model pipeline, or for big-data image evaluation for research. For example, Wasserthal et al demonstrate a sample application of their TotalSegmentator model for assessing the age dependency of organ volumes and attenuation on polytrauma CT for over 4000 patients (10). Furthermore, our model has demonstrated flexibility on disparate datasets and new modalities via transfer learning and/or fine tuning. Thus, MRAnnotator can be further adapted for novel applications via techniques such as transfer learning, fine tuning, few-shot learning, and zero-shot learning, or in

combination with other emerging novel techniques such as generative, semi-supervised, or self-supervised approaches.

Our study has several limitations. One limitation of our study is the use of a restricted selection of sequences from each study. Typically, an MRI study requires a variety of sequences to facilitate accurate diagnoses. Moreover, comprehensive MRI analyses often demand studies in multiple orientations, such as axial, sagittal, and coronal views, to ensure a thorough diagnosis. However, our research incorporated only a single view.

There are several avenues for future study. Firstly, we plan to incorporate additional anatomic regions, such as chest, cardiac, musculoskeletal, and brain, into our model and datasets. Secondly, we plan to investigate the utility of our model in the preparation of large-scale annotated datasets for the training of larger-scale models for medical imaging. Lastly, we plan to apply the data and models from this and future work towards the development of additional foundation models across the “spectrum of foundation models” set forth by Zhang and Metaxas (9), particularly larger-scale and more generalized foundation models.

In conclusion, we developed an MRI segmentation model that is easy to use, capable of segmenting 49 anatomic structures throughout the entire body, and generalizable to external imaging centers.

Figures

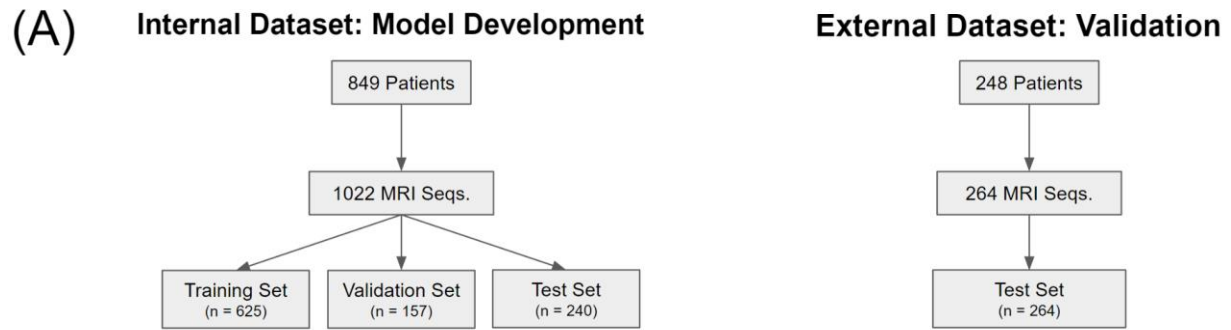


Figure 1: (A) Diagram of patient inclusion and sequences selection for dataset curation and annotation. (B) Diagram of the iterative model-assisted workflow for the annotation of structures.

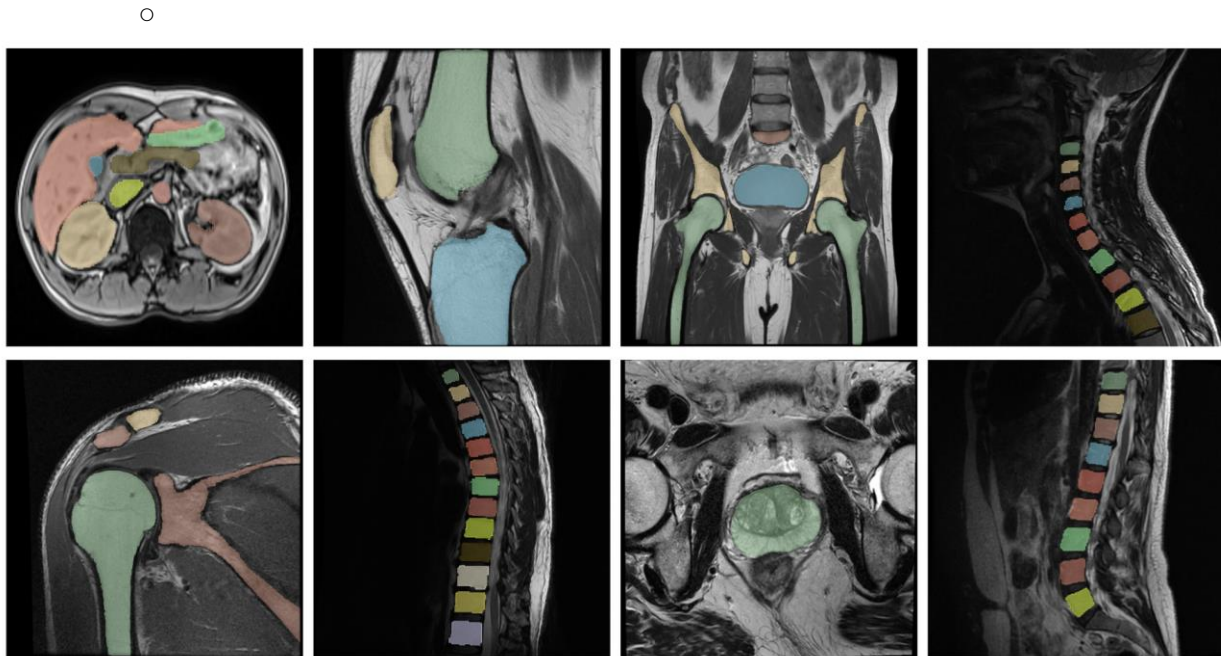


Figure 2: Examples of annotated anatomical regions across 49 classes include: in the first row, abdomen, knee, pelvis, cervical spine; in the second row, shoulder, thoracic spine, prostate, and lumbar spine.

References

1. Wang L, Wang H, Huang Y, et al. Trends in the application of deep learning networks in medical image analysis: Evolution between 2012 and 2020. *European Journal of Radiology*. 2022;146:110069. doi: 10.1016/j.ejrad.2021.110069.
2. Lundervold AS, Lundervold A. An overview of deep learning in medical imaging focusing on MRI. *Zeitschrift für Medizinische Physik*. 2019;29(2):102–127. doi: 10.1016/j.zemedi.2018.11.002.
3. Isensee F, Jaeger PF, Kohl SAA, Petersen J, Maier-Hein KH. nnU-Net: a self-configuring method for deep learning-based biomedical image segmentation. *Nat Methods*. Nature Publishing Group; 2021;18(2):203–211. doi: 10.1038/s41592-020-01008-z.
4. Montagnon E, Cerny M, Cadrin-Chênevert A, et al. Deep learning workflow in radiology: a primer. *Insights into Imaging*. 2020;11(1):22. doi: 10.1186/s13244-019-0832-5.
5. Mazurowski MA, Buda M, Saha A, Bashir MR. Deep learning in radiology: an overview of the concepts and a survey of the state of the art with focus on MRI. *J Magn Reson Imaging*. 2019;49(4):939–954. doi: 10.1002/jmri.26534.
6. Chen D, Liu S, Kingsbury P, et al. Deep learning and alternative learning strategies for retrospective real-world clinical data. *npj Digit Med*. Nature Publishing Group; 2019;2(1):1–5. doi: 10.1038/s41746-019-0122-0.
7. Willeminck MJ, Koszek WA, Hardell C, et al. Preparing Medical Imaging Data for Machine Learning. *Radiology*. Radiological Society of North America; 2020;295(1):4–15. doi: 10.1148/radiol.2020192224.
8. Moor M, Banerjee O, Abad ZSH, et al. Foundation models for generalist medical artificial intelligence. *Nature*. Nature Publishing Group; 2023;616(7956):259–265. doi: 10.1038/s41586-023-05881-4.
9. Zhang S, Metaxas D. On the challenges and perspectives of foundation models for medical image analysis. *Medical Image Analysis*. 2024;91:102996. doi: 10.1016/j.media.2023.102996.
10. Wasserthal J, Breit H-C, Meyer MT, et al. TotalSegmentator: Robust Segmentation of 104 Anatomic Structures in CT Images. *Radiology: Artificial Intelligence*. Radiological Society of North America; 2023;5(5):e230024. doi: 10.1148/ryai.230024.
11. Fauveau V, Sun S, Liu Z, et al. Discovery Viewer (DV): Web-Based Medical AI Model Development Platform and Deployment Hub. *Bioengineering*. Multidisciplinary Digital Publishing Institute; 2023;10(12):1396. doi: 10.3390/bioengineering10121396.
12. Ma J, He Y, Li F, Han L, You C, Wang B. Segment anything in medical images. *Nat Commun*. Nature Publishing Group; 2024;15(1):654. doi: 10.1038/s41467-024-44824-z.
13. Huo L, Hu X, Xiao Q, Gu Y, Chu X, Jiang L. Segmentation of whole breast and fibroglandular tissue using nnU-Net in dynamic contrast enhanced MR images. *Magnetic Resonance Imaging*. 2021;82:31–41. doi: 10.1016/j.mri.2021.06.017.
14. Isensee F, Jäger PF, Full PM, Vollmuth P, Maier-Hein KH. nnU-Net for Brain Tumor Segmentation. In: Crimi A, Bakas S, editors. *Brainlesion: Glioma, Multiple Sclerosis, Stroke and Traumatic Brain Injuries*. Cham: Springer International Publishing; 2021. p. 118–132. doi: 10.1007/978-3-030-72087-2_11.
15. Zou KH, Warfield SK, Bharatha A, et al. Statistical Validation of Image Segmentation Quality Based on a Spatial Overlap Index. *Acad Radiol*. 2004;11(2):178–189. doi: 10.1016/S1076-6332(03)00671-8.
16. Menze BH, Jakab A, Bauer S, et al. The Multimodal Brain Tumor Image Segmentation Benchmark (BRATS). *IEEE Trans Med Imaging*. 2015;34(10):1993–2024. doi: 10.1109/TMI.2014.2377694.
17. Weiner MW, Aisen PS, Jack CR, et al. The Alzheimer’s disease neuroimaging initiative: progress report and future plans. *Alzheimers Dement*. 2010;6(3):202–211.e7. doi: 10.1016/j.jalz.2010.03.007.
18. Liu C-F, Leigh R, Johnson B, et al. A large public dataset of annotated clinical MRIs and metadata of patients with acute stroke. *Sci Data*. Nature Publishing Group; 2023;10(1):548. doi: 10.1038/s41597-023-02457-9.

19. Kavur AE, Gezer NS, Barış M, et al. CHAOS Challenge - combined (CT-MR) healthy abdominal organ segmentation. *Medical Image Analysis*. 2021;69:101950. doi: 10.1016/j.media.2020.101950.
20. Ji Y, Bai H, Yang J, et al. AMOS: A Large-Scale Abdominal Multi-Organ Benchmark for Versatile Medical Image Segmentation. *arXiv*; 2022. doi: 10.48550/arXiv.2206.08023.
21. Li Y, Fu Y, Gayo IJMB, et al. Prototypical few-shot segmentation for cross-institution male pelvic structures with spatial registration. *Medical Image Analysis*. 2023;90:102935. doi: 10.1016/j.media.2023.102935.
22. Petersen SE, Matthews PM, Francis JM, et al. UK Biobank’s cardiovascular magnetic resonance protocol. *Journal of Cardiovascular Magnetic Resonance*. 2016;18(1):8. doi: 10.1186/s12968-016-0227-4.
23. Ding H, Sun C, Tang H, Cai D, Yan Y. Few-shot Medical Image Segmentation with Cycle-resemblance Attention. 2023 IEEE/CVF Winter Conference on Applications of Computer Vision (WACV). 2023. p. 2487–2496. doi: 10.1109/WACV56688.2023.00252.
24. Kondo S, Kasai S. Multi-Modality Abdominal Multi-Organ Segmentation with Deep Supervised 3D Segmentation Model. *arXiv*; 2022. doi: 10.48550/arXiv.2208.12041.

Supplementary

Table S1: Model segmentation accuracy on internal and external dataset holdout test sets for all classes.